J. Fluid Mech. (2008), *vol.* 608, *pp.* 275–296.
doi:10.1017/S0022112008002048 Printed in the United Kingdom

Underwater breathing: the mechanics of plastron respiration

M. R. FLYNN† AND JOHN W. M. BUSH

Department of Mathematics, Massachusetts Institute of Technology, 77 Massachusetts Avenue, Cambridge, MA 02139-4307, USA

(Received 11 July 2007 and in revised form 10 April 2008)

The rough, hairy surfaces of many insects and spiders serve to render them water-repellent; consequently, when submerged, many are able to survive by virtue of a thin air layer trapped along their exteriors. The diffusion of dissolved oxygen from the ambient water may allow this layer to function as a respiratory bubble or 'plastron', and so enable certain species to remain underwater indefinitely. Maintenance of the plastron requires that the curvature pressure balance the pressure difference between the plastron and ambient. Moreover, viable plastrons must be of sufficient area to accommodate the interfacial exchange of O_2 and CO_2 necessary to meet metabolic demands. By coupling the bubble mechanics, surface and gas-phase chemistry, we enumerate criteria for plastron viability and thereby deduce the range of environmental conditions and dive depths over which plastron breathers can survive. The influence of an external flow on plastron breathing is also examined. Dynamic pressure may become significant for respiration in fast-flowing, shallow and well-aerated streams. Moreover, flow effects are generally significant because they sharpen chemical gradients and so enhance mass transfer across the plastron interface. Modelling this process provides a rationale for the ventilation movements documented in the biology literature, whereby arthropods enhance plastron respiration by flapping their limbs or antennae. Biomimetic implications of our results are discussed.

1. Introduction

Strategies for water-repellence are identical in the plant and animal kingdoms, and have provided important guidance in the development of industrial superhydrophobic surfaces (Herminghaus 2000; Wagner *et al.* 2003; Otten & Herminghaus 2004; Abdelsalam *et al.* 2005; Chen *et al.* 2005; Shirtcliffe *et al.* 2006; Feng & Jiang 2006; Cao, Hu & Gao 2007; Nosonovsky 2007). Quite generally, a rough, waxy surface is presented that increases the energetic cost of wetting and so discourages fluid–solid contact (de Gennes, Brochard-Wayart & Quéré 2003). If a hydrophobic surface is sufficiently rough, water cannot penetrate the roughness elements, an intervening air layer persists, and the system is said to be in a Cassie state (Cassie & Baxter 1944). Such is the case for lotus leaves, that are known to be both water-repellent and self-cleaning owing to their complex surface roughness (Neinhuis & Barthlott 1997; Barthlott & Neinhuis 1997). Conversely, if the surface is sufficiently smooth or hydrophilic, a Wenzel state (Wenzel 1936) may obtain, in which water impregnates the roughness elements. While metastable Cassie states may arise (Lafuma & Quéré 2003; Cao *et al.* 2007), the general criterion for a Cassie state is that it be energetically

† Present address: Department of Mechanical Engineering, University of Alberta, Edmonton, AB T6G 2G8, Canada.

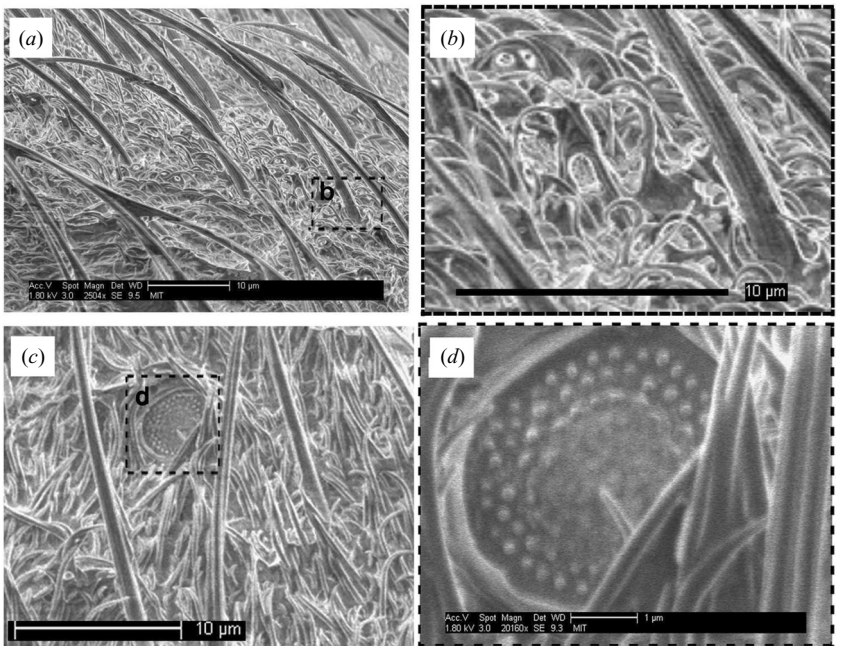

FIGURE 1. Scanning electron microscope images of the integument of the water-walking insect *Mesovelia*. (*a, b*) As with most water-walking insects, *Mesovelia* exhibits a two-tiered hair layer on its thorax (body cavity), with the inner layer, the microtrichia, supporting a plastron in case of submergence. (*c, d*) Note the spiracle, through which it breathes, nestled among the microtrichia. True aquatic insects are more often characterized by a narrow range of hair geometries (Thorpe & Crisp 1949). Images courtesy of M. Prakash.

favourable relative to the wetted Wenzel state. In terms of mechanics, maintenance of the Cassie state requires that the Laplace pressure generated by the intruding interface balance the applied pressure. For roughness characterized by a single length scale δ, this requirement for water-repellency may be simply expressed as $\sigma/\delta > \Delta p$ where σ is the surface tension and Δp is the pressure difference. We proceed by considering a physical system for which the maintenance of water-repellency is quite literally a matter of life and death.

Many aquatic and semi-aquatic arthropods (insects and spiders) are rendered water-repellent by virtue of a rough, waxy exterior festooned with hairs (Andersen 1977; Perez-Goodwyn 2007; Bush, Hu & Prakash 2008). The advantages of this integument are several-fold: it enables many species of insects and spiders to walk on water (Bush & Hu 2006), survive the impact of raindrops (Andersen 1977), and endure brief periods of submersion (Andersen & Polhemus 1976; Spence, Spence & Scudder 1980). Water-repellency is particularly pronounced among select species of insects (Schmidt-Nielsen 1975; Brown 1987) and spiders (Lamoral 1968; Stratton, Suter & Miller 2004; Schütz & Taborsky 2003) that occupy marine habitats. Breathing for such arthropods generally occurs through a series of spiracles, small surface openings typically located on the thorax (figure 1; Hinton & Jarman 1976). Consequently, when these creatures are submerged, their respiratory demands may be satisfied provided a thin layer of air is maintained along their body surface (figure 2; Thorpe & Crisp 1947*a, b, c*; Thorpe 1950). The air bubble serves as an external lung that exchanges O_2 and CO_2 with the surrounding water (de Ruiter *et al.* 1951). In many cases (Chaui-Berlinck, Bicudo & Monteiro 2001; Matthews & Seymour 2006), the respiratory function of

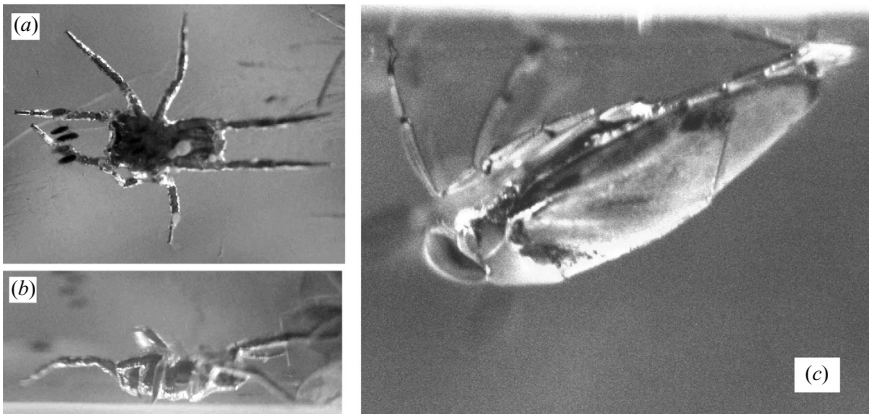

FIGURE 2. (*a*, *b*) The Fisher spider *Dolomedes triton*. The air layer along the Fisher spider's exterior is approximately 0.2 mm thick and is responsible its silvery sheen. The layer contributes to the spider's buoyancy and so facilitates re-surfacing; moreover, it serves as an O_2 supply. (Photograph courtesy of D. Hu.) (*c*) The backswimmer *Notonecta* hangs inverted from the free surface. Its respiratory bubble covers the bulk of its body.

this air bubble is limited so that it serves as a diminishing resource: the bubble volume decreases steadily over time and the arthropod can remain underwater only for a finite period. The creatures of particular interest to our study are those that can stay submerged indefinitely and are thus relieved, at least on respiratory grounds, from making regular ascents to the water surface. In this circumstance, the air bubble, or 'plastron', maintains a constant volume. Mass transfer across the plastron surface depends on the chemical gradient across the interface and so is particularly efficient in well-aerated water (Thorpe & Crisp 1947*b*; Rahn & Paganelli 1968).

By incorporating biological, chemical and mechanical considerations, a model of plastron dynamics is developed. Specifically conditions are identified for which a plastron may be maintained indefinitely with no deterioration of respiratory function. We shall demonstrate that the maximum dive depth of a plastron breather is limited by two constraints: the maintenance of water-repellency, and the creature's respiratory demands. While water-repellency is enhanced by a tall, tightly packed hair lattice, such a configuration may make it impossible for the arthropod to breathe, particularly near the free surface. Resolving the nature of the resulting tradeoff is the principal goal of our study. To this end, we develop a quantitative model that allows us to rationalize a number of poorly understood observations of plastron breathing reported in the biology literature. We consider an idealized geometry in which the plastron surface is supported by hairs lying parallel to the arthropod's body for which a two-dimensional hair lattice is appropriate. The pressure difference across the plastron surface determines its shape and so the interfacial area available for gas exchange. Building on the previous analyses of Ege (1918), Thorpe & Crisp (1947*a*, *b*, *c*, 1949), Hinton (1976), and others, the resulting coupling between plastron mechanics, surface and gas-phase chemistry is considered. Predictions are made for the range of environmental conditions over which plastron breathing is viable in a quiescent fluid.

Fluid flow is also critical to certain underwater breathers. The aquatic insect *Potamodytes tuberosus*, a relatively large freshwater beetle, inhabits shallow, fast-flowing streams on Africa's Gold Coast. Stride (1954) demonstrated that *Potamodytes*

tuberosus orients its body so as to create a stationary, cavitation bubble in its lee. As noted by Stride (1954) and examined in greater detail below, the cavitation bubble results from Bernoulli pressure lows resulting from large flow speeds. Indeed, Stride's field observations suggest that *Potamodytes tuberosus* relocates to more briskly flowing streams once the flow velocity in its local habitat drops below a well-defined critical value. Moreover, biologists have reported a variety of 'ventilation movements' whereby arthropods increase O_2 and CO_2 exchange by flapping their limbs for relatively brief periods (Brocher 1912*b*; de Ruiter *et al.* 1951; Gittelman 1975) or their antennae for extended periods (Brocher 1912*a*). In the case of the lake insect *Neoplea striola*, for example, such ventilation movements are observed as the insect emerges from its winter hibernation and needs to expand its plastron to support its increased metabolic activity (Gittelman 1975). In order to rationalize the above observations, we examine the role of fluid flow on underwater breathing, exploring both its direct influence through dynamic pressures and its indirect influence on boundary layer transport.

The paper is organized as follows. In § 2, we describe the simplified model geometry of the hair lattice and plastron interface. In § 3, we present a model of the gas-phase chemistry associated with plastron respiration. A detailed analysis of the resulting governing equations is given in § 4, where we derive criteria for viable plastron respiration in a static ambient. The role of dynamics is investigated in § 5. The biological implications and possible biomimetic applications of our study are discussed in § 6.

2. Plastron mechanics

To serve as an effective vehicle for gas exchange, a plastron must be securely affixed to those portions of the arthropod's body containing spiracles (figure 1). Thorpe & Crisp (1947*a*) and Crisp (1949) note that water-repellency of arthropod cuticle is enhanced when the hairs are equidistant from their neighbours and tilted so as to lie parallel to the plane of the surface. In certain species, the hair lattice density increases in the immediate neighbourhood of the spiracles so as to prevent spiracle flooding in the event of plastron collapse further afield; however, this complication will not be examined here. Plastron hairs typically form a series of inverted L-shapes: after rising perpendicular to the arthropod's body, the hairs execute a right-angle bend (figure 3*a*; Vogel 2006; Brocher 1912*a*, *b*; Thorpe & Crisp 1949; Hinton 1976; Andersen 1976, 1977). Although this hair configuration is not universal among plastron breathers (e.g. *Elmis maugei, Riolus cupreus, Phytobius velatus* – Thorpe & Crisp 1949), we shall adopt this idealized geometry here for the sake of simplicity.

It is noteworthy that arthropod integument is not entirely rigid, and that individual hairs may bend under the influence of capillary forces (Bush *et al.* 2008). Thorpe & Crisp (1947*a*) suggested that plastron stability may be jeopardized by the collapse of the plastron hairs; however, Hinton (1976) concluded that plastron hairs will only buckle at great depths (of order 400 m), and that plastrons are 'wetted long before there is any question of the collapse of the hair pile itself'. Moreover, Brocher (1912*a*, *b*) noted that there is a degree of overlap between adjacent plastron hairs, thus further contributing to the stability of the hair lattice (figure 3*a*). We thus proceed by assuming that the lattice geometry is fixed and independent of the ambient pressure. The implications of flexible cuticle for plastron stability are examined in § 6.

Figure 3 illustrates the idealized two-dimensional geometry of the hair lattice and plastron interface. The plastron is maintained against the pressure of the overlying fluid via surface tension. Hence, the liquid–gas interface is curved and has a shape

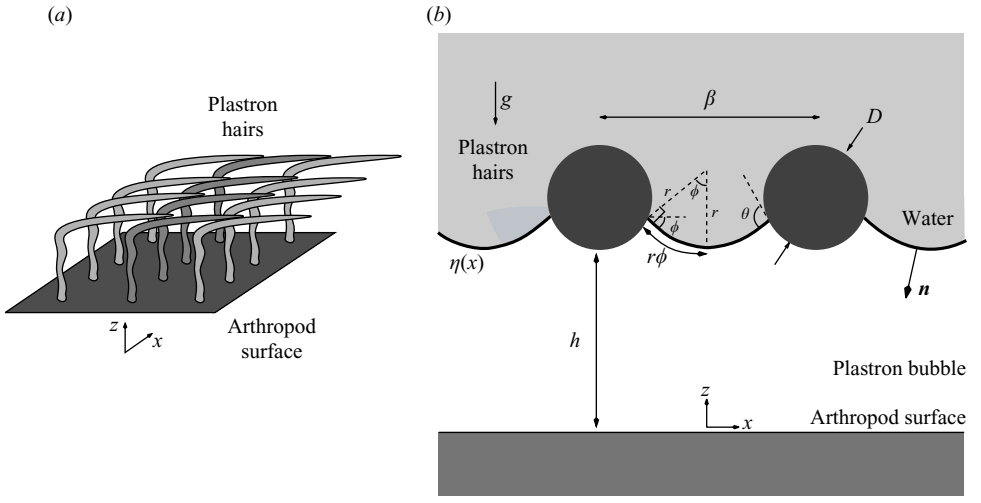

FIGURE 3. (*a*) The characteristic geometry of the plastron hair pile: bent hairs lie tangent to the body surface, optimizing water-repellency. (*b*) The idealized two-dimensional model geometry of the plastron hairs and interface.

satisfying the two-dimensional Young–Laplace equation

$$\frac{\Delta p}{\sigma} = -\nabla \cdot \boldsymbol{n} = \frac{\eta_{xx}}{\left(1+\eta_x^2\right)^{3/2}}, \tag{2.1}$$

subject to the boundary conditions

$$\eta_x(0) = 0, \qquad \eta_x\left(\tfrac{1}{2}[\beta - D\sin(\theta-\phi)]\right) = \tan\phi\,. \tag{2.2a, b}$$

From the reference coordinates defined in figure 3(*b*), it may be seen that boundary condition (2.2*a*) is applied at a point equidistant between adjacent hydrophobic hairs, (2.2*b*) at the triple point. Here $\sigma \sim 72\,\mathrm{dyn\,cm^{-1}}$ is the surface tension, $\boldsymbol{n}$ the unit normal vector, $\eta(x)$ the interface height, β the centre-to-centre spacing between adjacent hairs, D the hair diameter and ϕ the angle the interface makes to the horizontal at the point of contact with the hydrophobic hairs. This angle depends on the pressure drop across the plastron interface, $\Delta p \equiv p - p_{bub}$. In what follows, we fix the equilibrium contact angle to be $\theta = 105^\circ$, a value representative of arthropod cuticle (Holdgate 1955; Perez-Goodwyn 2007; Vogel 2006).

With the coordinate system origin placed between neighbouring hairs as in figure 3(*b*), (2.1) can be integrated with respect to x and the boundary condition (2.2*a*) applied to yield

$$\eta_x = \frac{x}{\sqrt{(\sigma/\Delta p)^2 - x^2}}, \tag{2.3}$$

where the pressure drop across the interface can be written as

$$\Delta p \equiv p - p_{bub} = \frac{\sigma}{r}.$$

Here r denotes the radius of curvature of the interface, which can be expressed in non-dimensional form as

$$\frac{r}{\beta} = \frac{1}{2\sin\phi}\left[1 - \frac{D}{\beta}\sin(\theta-\phi)\right]. \tag{2.4}$$

The above results show that bubble collapse will occur when $\Delta p > \sigma/r_{min}$ where, for a fixed hair geometry, the minimum radius of curvature, r_{min}, can be deduced from (2.4) by varying over the angle ϕ. In this circumstance, the hydrophobic hairs are unable to retain the plastron against the surface of the insect, so the bubble is displaced by an advancing front of water (Bico, Thiele & Quéré 2002). To quantify this criterion for plastron collapse, some measure of the bubble pressure, p_{bub}, is necessary. We shall therefore return to consider the mechanical stability of the plastron following § 3, where we calculate p_{bub} from the gas-phase chemistry.

Equation (2.3) can be further integrated to obtain the interface shape. For a prescribed hair geometry, we can therefore determine the total vertical deflection of the interface. This in turn specifies the minimum height of the hair lattice, $h_{min} = \eta(x = 0)$, required to prevent the interface from touching down under the influence of the applied pressure:

$$h_{min} = r\,(1 - \cos\phi) - \frac{D}{2}\,[1 - \cos\,(\theta - \phi)], \tag{2.5}$$

where h is defined in figure 3(b). Note that in the limit of a sparse lattice, $D/\beta \ll 1$, (2.5) can be simply expressed as

$$h_{min} = \frac{\beta}{2}. \tag{2.6}$$

For fixed D and β, the interface is uniquely prescribed by r/β and ϕ. Figure 4(a) shows the dependence of r/β and ϕ on the non-dimensional hair diameter, D/β. As $r/\beta \to \infty$, the interface becomes flat and therefore $\phi \to 0$. The radius of curvature becomes vanishingly small as $D/\beta \to 1$ and $\phi \to \theta - 90^\circ$. Figure 4($a$) shows that r/β is not, in general, a monotonic function of the interface angle, ϕ. When the interface is deflected to its maximum possible extent, adjacent interfaces located on opposite sides of a given hydrophobic hair are just at the point of overlap such that $r = \beta/2$ and

$$\frac{D}{\beta}\sin\,(\theta - \phi) + \sin\phi = 1, \tag{2.7}$$

which defines the maximum possible interface angle, $\phi_{max} < \theta$, as a function of the geometric parameter D/β.

Because the interface is assumed to be a circular arc as illustrated schematically in figure 3(b), the interface or gill length between adjacent hydrophobic hairs is given by $\ell = 2\phi r$; thus,

$$\frac{\ell}{\beta} = 2\phi\,\frac{r}{\beta} = \frac{A}{A_{\mathrm{p}}} \tag{2.8}$$

prescribes the relative magnitudes of the plastron surface area, A, and the underlying planar area, A_{p}. We note that A_{p} is much easier to estimate than A because the latter depends on the interfacial curvature.

The dimensionless gill length, ℓ/β, may be greater than unity if the interface is sharply curved and much smaller than unity if the interface curvature is relatively small and the hair lattice tightly packed, i.e. $D/\beta \to 1$. Thus ℓ/β may vary over a broad range and is not simply an $O(1)$ quantity (figure 4b). When ℓ/β is relatively small, the respiration surface area is small and thus the exchange of O_2 and CO_2 across the plastron interface is restricted. Respiration imposes a minimum gill length, below which the plastron becomes devoid of O_2 in steady state. Figure 4(a, b) therefore represents idealizations; real plastrons are better represented by figure 4(c, d), in which the minimum gill length required for respiration is prescribed by the vertical

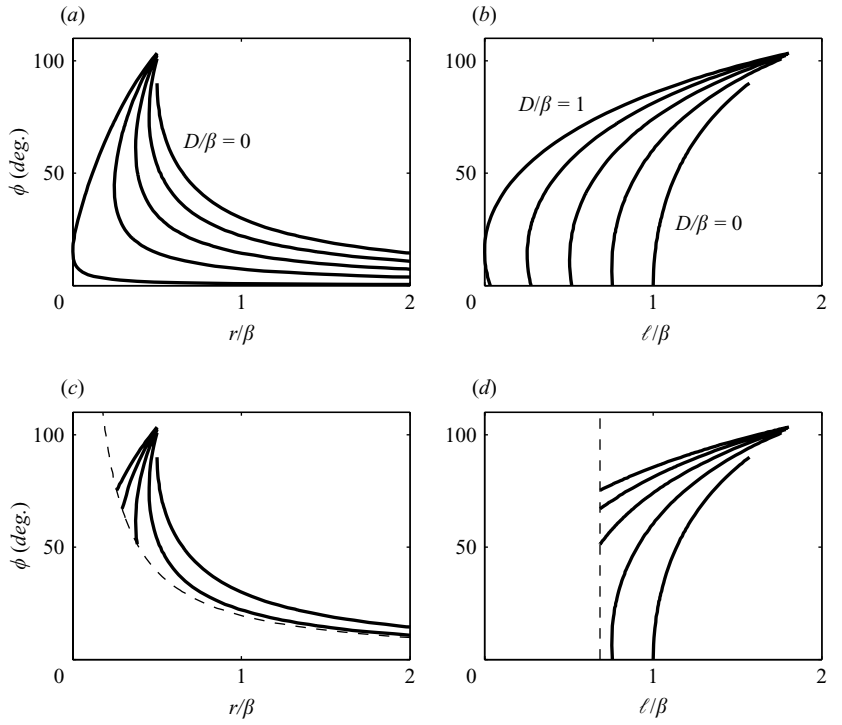

FIGURE 4. Interface angle, ϕ, as a function of the non-dimensional radius of curvature, r/β, and the dimensionless gill length, ℓ/β, for $D/\beta = 0$, 0.25, 0.5, 0.75, 1 where D and β are defined in figure 3(*b*). (*a*, *b*) Zero respiration rate. (*c*, *d*) Finite respiration rate. In (*c*, *d*), there is a minimum interface length and a corresponding (ϕ-dependent) critical radius of curvature, shown by the dashed lines.

dashed line. Corresponding to this minimum of ℓ/β, figure 4(*c*) shows the critical non-dimensional radius of curvature. As these results make clear, underwater breathing via plastrons is characterized by both a maximum and minimum interface angle, where, in general, $\phi_{max} < \theta$ and $\phi_{min} > 0^\circ$. For $\phi > \phi_{max}$ interface overlap will occur. For $\phi < \phi_{min}$, the plastron will be of insufficient area to accommodate the gas exchange required for respiration.

Figure 4(*c*) shows that a plastron must be both mechanically stable so that the Laplace pressure, σ/r, balances $\Delta p \equiv p - p_{bub}$, and be of sufficient surface area to meet the respiratory demands of the arthropod. Plastrons with $\phi_{min} \leqslant \phi \leqslant \phi_{max}$ that are both stable and functional as a gill are termed viable and can be maintained indefinitely without long-term deterioration. Whereas plastron stability favours a tightly packed hair lattice, the plastron surface area may become too small to support respiration with $D/\beta \to 1$, especially close to the free surface where the ambient pressure causes only slight interfacial deflections.

3. Gas-phase chemistry

The time-dependent exchange of gases from the plastron to the surrounding water column can be described using the three-component model summarized in Thorpe & Crisp (1947*b*) and Rahn & Paganelli (1968). It is assumed that the time rate of change of the bubble volume depends on the respiration rate, the plastron surface area and

the difference of concentrations of the chemical components across the liquid–gas interface. Thus

$$\dot{V}_{O_2} = \frac{A\,(\alpha\,\widehat{D})_{O_2}}{\bar{\delta}_{O_2}}\,(x_{O_2}\,\mathscr{H}_{O_2} - p_{O_2}) - q, \tag{3.1}$$

$$\dot{V}_{N_2} = \frac{A\,(\alpha\,\widehat{D})_{N_2}}{\bar{\delta}_{N_2}}\,(x_{N_2}\,\mathscr{H}_{N_2} - p_{N_2}), \tag{3.2}$$

$$\dot{V}_{CO_2} = \frac{A\,(\alpha\,\widehat{D})_{CO_2}}{\bar{\delta}_{CO_2}}\,(x_{CO_2}\,\mathscr{H}_{CO_2} - p_{CO_2}) + q, \tag{3.3}$$

where q is the rate of O_2 consumption and CO_2 production, A is the plastron surface area and V_j and p_j are, respectively, the volume and partial pressure of chemical constituent j in the plastron. Moreover, x_j is the dissolved gas concentration, $\mathscr{H}_j$ the corresponding Henry's law constant, $\bar{\delta}_j$ the spatially averaged (mass diffusion) boundary layer thickness, α_j the solubility and $\widehat{D}_j$ the diffusion coefficient. In the biology literature, it is customary to group the latter three variables together in the form of a constituent-dependent 'invasion coefficient':

$$\mathscr{J}_j \equiv \frac{(\alpha\,\widehat{D})_j}{\bar{\delta}_j}\,. \tag{3.4}$$

In equations (3.1)–(3.3), we assume that, as in Rahn & Paganelli (1968) and Geankoplis (1993), the rate-limiting step in mass exchange is diffusion through a thin, poorly mixed layer of water adjoining the plastron. Conversely, it is assumed that p_{O_2}, p_{N_2} and p_{CO_2} do not vary over the spatial extent of the plastron. Although this is only an approximation, it is consistent with the observation of Thorpe & Crisp (1947*b*) that gas-phase concentrations within the plastron are 'fairly uniform' (see also Hinton & Jarman 1976).

Equations (3.1)–(3.3) can be rearranged to solve for the partial pressure of each chemical constituent. Thus for example,

$$p_{O_2} = x_{O_2}\,\mathscr{H}_{O_2} - \left(\frac{\dot{V}_{O_2} + q}{A\,\mathscr{J}_{O_2}}\right). \tag{3.5}$$

By Dalton's law, the total pressure within the plastron is the sum of the partial pressures of all of its chemical components:

$$p_{bub} = p_{H_2O} + p_{O_2} + p_{N_2} + p_{CO_2}, \tag{3.6}$$

where p_{H_2O} denotes the partial pressure of water vapour. The time-varying bubble pressure is thus given by

$$p_{bub} = p_{H_2O} + x_j\,\mathscr{H}_j - \left(\frac{\dot{V}_{O_2} + q}{A\,\mathscr{J}_{O_2}}\right) - \frac{\dot{V}_{N_2}}{A\,\mathscr{J}_{N_2}} - \left(\frac{\dot{V}_{CO_2} - q}{A\,\mathscr{J}_{CO_2}}\right), \tag{3.7}$$

where, for notational convenience, Einstein's summation convention is applied, i.e.

$$x_j\,\mathscr{H}_j = x_{O_2}\,\mathscr{H}_{O_2} + x_{N_2}\,\mathscr{H}_{N_2} + x_{CO_2}\,\mathscr{H}_{CO_2}\,.$$

Equation (3.7) can be further simplified by noting that under normal conditions, $p_{H_2O} \ll p_{bub}$ and $\mathscr{J}_{CO_2} \simeq 20 \times \mathscr{J}_{O_2}$ (Rahn & Paganelli 1968). Therefore, to leading order

$$p_{bub} \simeq x_j\,\mathscr{H}_j - \left(\frac{\dot{V}_{O_2} + q}{A\,\mathscr{J}_{O_2}}\right) - \frac{\dot{V}_{N_2}}{A\,\mathscr{J}_{N_2}}\,. \tag{3.8}$$

Once steady state has been achieved, $\dot{V}_{N_2} = \dot{V}_{O_2} = 0$, so (3.8) reduces to

$$p_{bub} \simeq x_j \mathscr{H}_j - \frac{q}{A \mathscr{J}_{O_2}}. \tag{3.9}$$

Because $q > 0$, one can identify

$$p_{bub} < x_j \mathscr{H}_j \tag{3.10}$$

as a fundamental requirement for plastron stability. The concentrations of dissolved O_2, N_2 and CO_2 often depend strongly on the hydrostatic pressure, the degree of photosynthetic and biological activity, or chemical reactions with the underlying sediment, and therefore frequently exhibit complex spatial, diurnal and seasonal variability (Dokulil 2005). Sidestepping such complications, we note that in many cases of biological relevance (e.g. shallow lakes with low biological productivity), $x_j \mathscr{H}_j \lesssim p_{atm}$. Because the bubble pressure is typically subatmospheric, plastron breathers do not require any of the specialized biological adaptations used by fish to breath at high pressures (Vogel 2006).

Obviously $p_j > 0$; hence, at steady state, (3.5) requires that

$$x_{O_2} \mathscr{H}_{O_2} > \frac{q}{A \mathscr{J}_{O_2}}, \tag{3.11}$$

which is the basic criterion for plastron functionality. For a given water chemistry, (3.11) places an upper bound on the rate of O_2 consumption, q, or equivalently a lower bound on the interface area, A. Specifically, (2.8) and (3.11) indicate that $p_{O_2} > 0$ provided

$$\Lambda \equiv \frac{x_{O_2} \mathscr{H}_{O_2} A_p \mathscr{J}_{O_2}}{q} > \frac{1}{\ell/\beta}, \tag{3.12}$$

where the non-dimensional parameter Λ prescribes the dissolved O_2 content of the water column relative to the respiration rate per unit planar area. One expects Λ to be relatively large in well-aerated streams so that a functional plastron can be maintained over a wide expanse of the water column (figure 4*a*, *b*). By the same token, one expects Λ to be relatively small in deep stagnant lakes, where a functional plastron can only be maintained over a restricted range of depths (figure 4*c*, *d*).

4. Plastron viability

4.1. *Mechanical stability*

The plastron is mechanically stable provided an interface shape exists that satisfies the normal stress balance: $\Delta p \equiv p - p_{bub} = \sigma/r$. At steady state, $\dot{V}_j = 0$, the bubble pressure may be expressed as (3.9) and the ambient pressure as $p = p_{atm} + \rho g H$ where ρ is the water density, $g = 9.8\,\mathrm{m\,s^{-2}}$ the gravitational acceleration and H the dive depth. The normal stress balance thus takes the form:

$$p_{atm} + \rho g H - x_j \mathscr{H}_j + \frac{q}{A \mathscr{J}_{O_2}} = \frac{\sigma}{r}. \tag{4.1}$$

When steady conditions cannot be assumed, the pressure is expressed by (3.8) and the criterion for mechanical stability takes the form:

$$p_{atm} + \rho g H - x_j \mathscr{H}_j + \frac{q}{A \mathscr{J}_{O_2}} = \frac{\sigma}{r} - \frac{\dot{V}_{O_2}}{A \mathscr{J}_{O_2}} - \frac{\dot{V}_{N_2}}{A \mathscr{J}_{N_2}}. \tag{4.2}$$

An arthropod with a stable plastron at its maximum dive depth may thus attain a transient stability at still greater depths provided $\dot{V}_{O_2} < 0$ or $\dot{V}_{N_2} < 0$. In this case, however, the plastron is compressed and the corresponding diminution of bubble volume may lead to plastron collapse.

In the remainder of our study, we shall focus on the steady-state condition $\dot{V}_j = 0$. We thus identify the range of environmental conditions in which (i) the stability condition (4.1) is satisfied, and (ii) the plastron is of sufficient area for respiration. Consistent with the nomenclature of § 2, a viable plastron is one that satisfies both conditions (i) and (ii). Non-dimensionalizing (4.1) yields

$$Bo + \Delta = \frac{1}{r/\beta} - \frac{\mathcal{Q}}{\ell/\beta}, \tag{4.3}$$

where

$$Bo = \frac{\rho\, g\, H}{\sigma/\beta}, \qquad \mathcal{Q} = \frac{q}{A_p\, \mathscr{J}_{O_2}(\sigma/\beta)}, \qquad \Delta = \frac{p_{atm} - x_j\, \mathscr{H}_j}{\sigma/\beta}. \tag{4.4a–c}$$

Here, Bo is the Bond number, which prescribes the non-dimensional dive depth. Furthermore, $\mathcal{Q}$ and Δ denote, respectively, the non-dimensional respiration rate and saturation pressure deficit. Supposing that O_2 demand varies as the two-thirds power of animal volume (McMahon & Bonner 1985) suggests that $\mathcal{Q}$ is independent of the arthropod size. This conclusion must be applied with care, however, because arthropod respiration does not universally scale as $q \sim \text{volume}^{2/3}$ (Gittelman 1975). Moreover, as suggested by Thorpe & Crisp (1949) and Gittelman (1975), q is expected to vary by an order of magnitude depending on the arthropod's level of activity; for example, q is substantially reduced during periods of hibernation. Finally, while $\mathcal{Q} > 0$, Δ can be either positive or negative corresponding, respectively, to sub- and super-saturation with respect to the atmosphere.

4.2. *Viability*

Figure 5 shows solutions to the plastron stability equation (4.3) for various D/β and $\mathcal{Q}$. The finite range of r and ℓ over which the plastron is viable, being mechanically stable while satisfying the arthropod's respiratory requirements, are precisely defined in equations (2.4), (2.7), (2.8) and (3.12). The curves of figure 5 are shown only over this range. When there are no respiratory demands on the creature, $\mathcal{Q} = 0$, there is no minimum gill length required for respiration, and no minimum dive depth: $\min(Bo + \Delta) = 0$. As expected the maximum dive depth (as indicated by the stars) increases monotonically with D/β. The latter trend also applies when $\mathcal{Q} > 0$ (figure 5*b–d*); however, as is obvious from (4.3), plastron stability is reduced by respiration. We note that for a fixed water chemistry, there are typically two values of r/β corresponding to a particular non-dimensional dive depth, Bo. This degeneracy is analogous to the non-unique Cassie states that have been documented in the case of a hydrophobic surface with sinusoidal micro-topography (Carbone & Mangialardi 2005). Notwithstanding this geometric distraction, each of the curves of figure 5 exhibits a well-defined maximum and minimum. The discussion can therefore be simplified by computing, for a given D/β and $\mathcal{Q}$, the maximum or minimum possible values of $Bo + \Delta$ (corresponding to the maximum or minimum dive depths for a fixed water chemistry).

We note that the radius of curvature that maximizes $Bo + \Delta$ does not necessarily coincide with the minimum possible value of r/β. Consider for example the middle curves of figures 4(*c*) and 5(*d*), corresponding to $D/\beta = 0.5$ and $\mathcal{Q} = 1$. In figure 4(*c*),

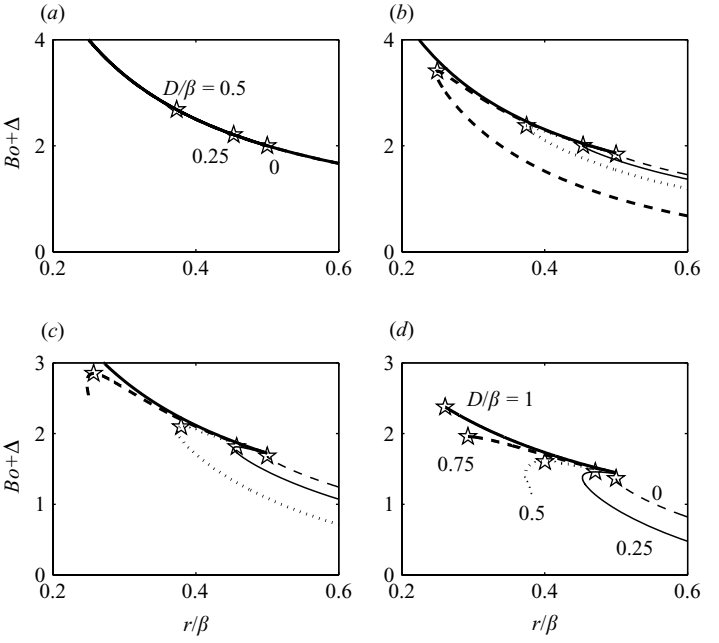

FIGURE 5. $Bo + \Delta$ versus r/β where Bo and Δ are, respectively, the dimensionless dive depth and saturation pressure deficit (see (4.4a, c)) and r/β is the dimensionless radius of curvature defined by (2.4). Different curves correspond to different hair geometries, i.e. $D/\beta = 0$, 0.25, 0.5, 0.75 and 1. Stars indicate the maximum of each curve. (a) $\mathcal{Q} = 0$, (b) $\mathcal{Q} = 0.25$, (c) $\mathcal{Q} = 0.5$ and (d) $\mathcal{Q} = 1$, where $\mathcal{Q}$ is the non-dimensional respiration rate defined by (4.4b). In each case, $x_{O_2}\mathscr{H}_{O_2}/(\sigma/\beta) = 1.46$ corresponding, for example, to a centre-to-centre hair spacing of 10 μm and an O_2 saturation fraction of 50 %. Consequently $\Lambda \to \infty$, $\Lambda = 5.85$, 2.92 and 1.46, respectively, in (a) to (d), where Λ is defined by (3.12). The Λ value used to generate (d) coincides with that used to generate figure 4(c, d).

r/β achieves a minimum value of 0.373, while in figure 5(d), $Bo + \Delta$ achieves a maximum value of 1.60 when $r/\beta = 0.401$. This nuance was overlooked by Crisp (1949) yet is fundamental to characterizing the role of respiration in plastron dynamics. Consistent with (4.3), it reflects the fact that $Bo + \Delta$ is a function of both the Laplace pressure and the pressure drop associated with respiration, the latter depending explicitly on the gill length, ℓ/β.

Figure 5 may be applied to determine the range of environmental conditions that guarantee plastron viability. Consider for example the curve of figure 5(d) corresponding to $D/\beta = 0.25$ and $\mathcal{Q} = 1$. A viable plastron may be maintained between $Bo + \Delta = 0$ and $Bo + \Delta = 1.46$. For $Bo + \Delta > 1.46$, the bubble pressure will exceed its maximum steady value, forcing the plastron to become unstable to diffusion and eventually collapse. This process can be arrested only by returning to shallower or better aerated waters. For the top curve of figure 5(d), where $D/\beta = \mathcal{Q} = 1$, $\max(Bo + \Delta) = 2.38$ is realized when $r/\beta = 0.261$. Mechanical stability cannot be maintained for $Bo + \Delta > 2.38$, while plastron functionality cannot be maintained for $r/\beta < 0.261$. The minimum dive depth, realized as $r/\beta \to 1/2$, is given by $\min(Bo + \Delta) = 1.45$, suggesting that a viable plastron may be untenable in near-surface waters. As these examples illustrate, plastron viability is, in general, constrained by two factors: (i) the Laplace pressure must balance the pressure drop across the interface, and (ii) the O_2 concentration within the plastron must remain non-zero.

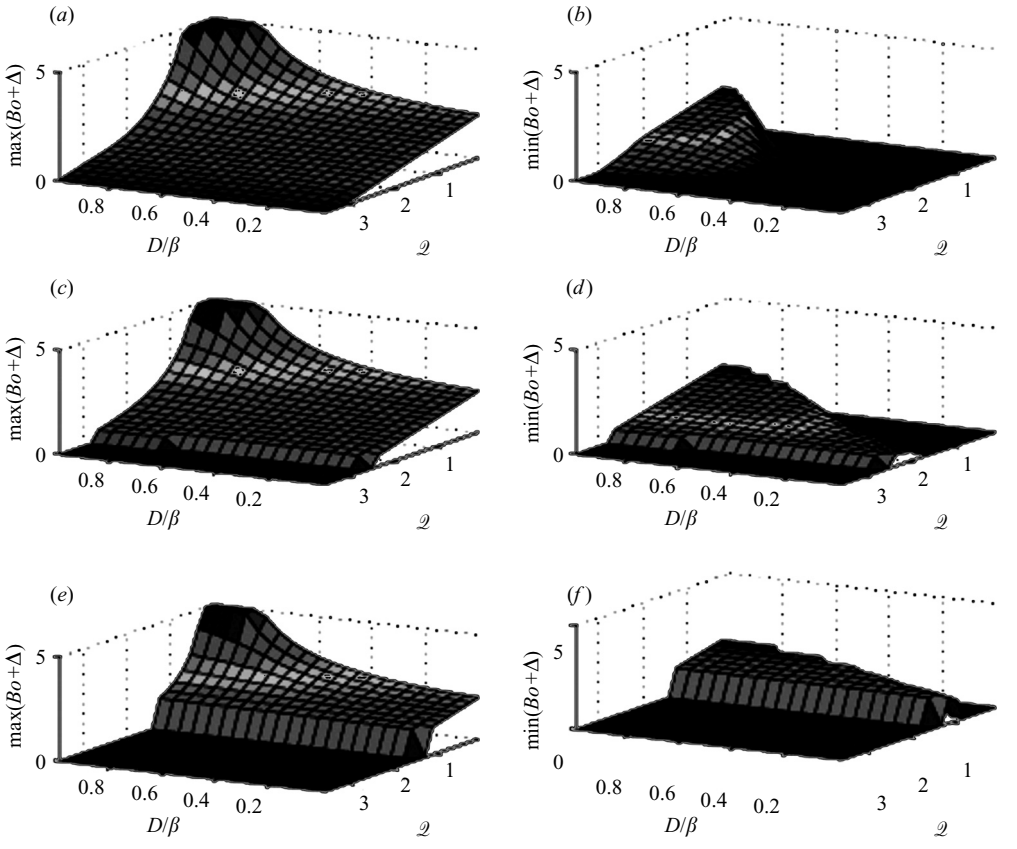

FIGURE 6. Maximum and minimum permissible values of $Bo + \Delta$ versus D/β and $\mathcal{Q}$ where Bo and Δ are, respectively, the dimensionless dive depth and saturation pressure deficit (see (4.4*a, c*)), $\mathcal{Q}$ is the dimensionless respiration rate defined by (4.4*b*) and D and β are the geometric parameters defined in figure 3(*b*). (*a*, *b*) $x_{O_2}\mathscr{H}_{O_2}/(\sigma/\beta) = 2.92$; (*c*, *d*) $x_{O_2}\mathscr{H}_{O_2}/(\sigma/\beta) = 1.46$; (*e*, *f*) $x_{O_2}\mathscr{H}_{O_2}/(\sigma/\beta) = 0.73$. Dissolved O_2 concentrations correspond to a centre-to-centre hair spacing of 10 μm and a water saturation fraction of 10%, 50% and 25%, respectively. For clarity of presentation, data corresponding to $\max(Bo + \Delta) > 5$ and $\min(Bo + \Delta) < 0$ are not shown. The lower plateaux indicated in (*c*) and (*e*) delineate areas in which (3.11) cannot be satisfied for any choice of r/β: a functional plastron cannot exist in these regions.

$\text{Min}(Bo+\Delta)$ and $\max(Bo+\Delta)$ are shown in figure 6 for a range of D/β and $\mathcal{Q}$ where each horizontal pair of figures corresponds to a different concentration of dissolved O_2 in the water column. Consistent with the discussion of figure 5, plastron-breathing arthropods can maintain a permanent physical gill only between the shaded surfaces. The general trend of $\max(Bo + \Delta)$ decreasing with increasing respiration rate, $\mathcal{Q}$, and lattice spacing, β, is evident in figure 6(*a, c, e*). In general there exists a minimum $(Bo+\Delta)$ that follows similar trends (figure 6*b, d, f*). Arthropods having a large demand for O_2 relative to body area will have great difficulty maintaining a stable physical gill at any appreciable depth. As indicated by figure 6(*e, f*), the situation is especially tenuous in poorly aerated waters for which no interface geometry can sustain a positive O_2 concentration according to (3.11). These constraints on plastron viability have important implications *vis-à-vis* biomimetic applications of plastron respiration to be discussed in § 6.

Species	Hair diameter, D(μm)	Spacing between adjacent hairs, β (μm)	Lattice height, h(μm)	Source
Stenelmis crenata	0.2	0.5 – 0.6	3–5	Thorpe & Crisp (1949)
Aphelocheirus aestivalis	0.4	0.5	3	Hinton (1976)
Elsianus aequalis	0.8	1.8 – 2.0	12	Thorpe & Crisp (1949)
Macrelmis corisors	1.0	1.6 – 1.8	16	Thorpe & Crisp (1949)
Haemonia mutica	2.0	2.5	14	Thorpe & Crisp (1949)

TABLE 1. Hair lattice geometries for a variety of aquatic insects capable of sustained plastron breathing.

While a rudimentary application of Laplace's equation suggests that the influence of a large metabolic rate on decreasing p_{bub} might be offset by expanding the hair diameter so that the hair lattice becomes more tightly packed, careful inspection of figure 6(a, c, e) shows that such is not necessarily the case. For $\mathcal{Q} \gtrsim 1$, increasing D yields a paltry gain in the maximum dive depth, which is given by $H_{max} = \sigma \max(Bo)/(\rho\, g\, \beta)$ (see (4.4a)). H_{max} depends strongly on β; therefore, decreasing the spacing between adjacent hydrophobic hairs does allow for notably deeper dives. As demonstrated by figure 6, however, $\max(Bo + \Delta)$ and $\min(Bo + \Delta)$ typically change in tandem. Therefore, as suggested by figure 4, arthropods capable of surviving at great depths may find, paradoxically, that their plastrons become ineffective at shallower depths, where the plastron interface is of insufficient surface area to meet their respiratory demands. Taken together, these observations may help to rationalize the wide range of reported hair lattice geometries, examples of which are provided in table 1.

4.3. *Biological case studies*

Our developments provide insight into the behaviour of the pygmy backswimmer *Neoplea striola*, a lake insect studied by Gittelman (1975). During the late autumn, as the water temperature decreases and dissolved gas concentration increases, *Neoplea striola* enters a state of winter hibernation. Because its basal metabolic rate is very low, *Neoplea striola* remains submerged for several months using a small thoracic plastron to satisfy its modest respiratory needs. The insect emerges from hibernation during spring once the water temperature reaches 10 to 12 °C and uses the ventilation movements documented in § 1 to rapidly increase the volume of its respiratory bubble. However, the resulting increase of the plastron surface area is not sufficient to compensate for the decrease in x_{O_2} and increase in q: when swimming actively in relatively warm water, the insect will asphyxiate unless it makes periodic ascents to the free surface to replenish this air store.

The utility of (4.3) is further demonstrated by examining the range of dive depths attainable by a particular insect with a fixed hair geometry. We focus specifically on the freshwater aquatic insect *Haemonia mutica* that maintains plastron bubbles along portions of its thorax, abdomen, head and long antennae (Thorpe & Crisp 1949). As reported by Doyen (1976), *Haemonia mutica* is a relatively slow-moving insect that occupies relatively still and densely vegetated marine environments.

Using reported values for the rate of O_2 consumption, q, and the planar area, A_p, of plastron in contact with *Haemonia mutica* (Thorpe & Crisp 1949) together with a representative value for the invasion coefficient of O_2 in stagnant water

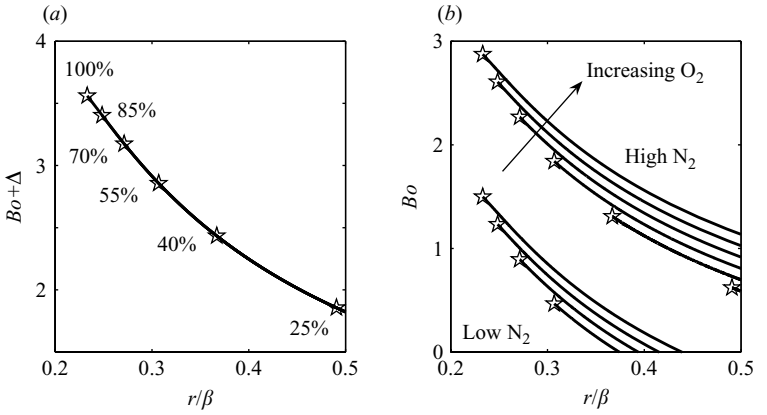

FIGURE 7. (*a*) $Bo+\Delta$ versus the dimensionless radius of curvature, r/β, where Bo and Δ denote, respectively, the dimensionless dive depth and saturation pressure deficit (see (4.4*a*, *c*)) and r/β is given by (2.4). Overlapping curves show the influence of the dissolved O_2 concentration for O_2 saturation fractions of 25 %, 40 %, 55 %... 100 %. The maximum of each curve is indicated by a star. (*b*) Analogous Bo versus r/β curves for low (25 %) and high (75 %) N_2 saturation fractions. Figures are representative for *Haemonia mutica* for which $D=2.0\,\mu\text{m}$, $\beta=2.5\,\mu\text{m}$, $q=3.9\times10^{-12}\,\text{m}^3\,\text{s}^{-1}$ and $A_p=1.2\times10^{-5}\,\text{m}^2$ (Thorpe & Crisp 1949).

($\mathscr{J}_{O_2}=3.5\times10^{-11}\,\text{m}^3\text{N}^{-1}\,\text{s}$; Rahn & Paganelli 1968), it can be shown from (3.12) that a functional plastron (i.e. $p_{O_2}>0$) requires a dissolved O_2 concentration, $x_{O_2}\mathscr{H}_{O_2}$, of at least 5.16 kPa, corresponding to an O_2 saturation fraction of 24.2%. Figure 7*a* shows $Bo+\Delta$ as a function of r/β for O_2 saturation fractions of 25%, 40%, 55% ... 100%. When x_{O_2} is small, there is very little difference between $\max(Bo+\Delta)$ and $\min(Bo+\Delta)$; however, the difference increases with increasing x_{O_2}. As a result, low ambient O_2 concentrations are associated with a relatively narrow range of dive depths. This dependence is illustrated graphically by figure 7(*b*), which shows Bo as a function of r/β. Figure 7(*b*) is similar to figure 7(*a*) except that the ordinate consists only of the non-dimensional dive depth, Bo, i.e. the contribution of the saturation pressure deficit, Δ, has been removed. It is assumed that x_{CO_2} is negligible while x_{N_2} is fixed at either 25% or 75% of its saturation value. Although we neglect the depth dependence of gas concentration, figure 7(*b*) offers two important insights. First, the maximum and minimum dive depths are sensitive to the concentration of dissolved N_2 in the water column: when x_{N_2} is relatively large, a viable plastron can be maintained at greater depths. This result is consistent with the classic experiment of Ege (1918) who observed that the dive times of insects are greatly increased if their plastron is composed of both O_2 and N_2 rather than pure O_2. Second, as x_{O_2} is progressively decreased, *Haemonia mutica* will eventually have to rise in the water column. This deduction is consistent with the observation of Thorpe & Crisp (1949): "*Haemonia*... tends to climb upwards when the aquarium is not well aerated... If conditions in the aquarium are allowed to get very bad it may even climb out".

5. The influence of dynamics

5.1. *Dynamic pressure*

The preceding discussion has focused on static conditions where the external flow velocity, U, is negligible. As noted in § 1, however, a number of species rely critically

on an ambient flow for underwater breathing. To incorporate flow effects into the governing equations, (4.3) may be re-written as

$$Bo + \Delta - We = \frac{1}{r/\beta} - \frac{\mathscr{Q}}{\ell/\beta}, \tag{5.1}$$

where the Weber number, *We*, is defined as

$$We = \frac{Eu\,\rho\,U^2}{\sigma/\beta}. \tag{5.2}$$

Here *Eu* is the Euler number that characterizes dynamic pressure variations along the arthropod's body. Because $Eu_{max} \sim 1$ (Kundu 1990), the minimum requirements for the dynamic pressure to affect plastron stability can be written as

$$\frac{U^2}{g\,H} \gtrsim 1, \qquad \frac{\rho\,U^2}{|p_{atm} - x_j\,\mathscr{H}_j|} \gtrsim 1. \tag{5.3}$$

These conditions are likely to be satisfied only for arthropods that inhabit shallow, fast-moving water. Even in relatively brisk currents, the dynamic pressure contribution is easily annulled by a minor drop in the dissolved gas concentration. For example with $U = 1\,\mathrm{m\ s^{-1}}$, $\rho\,U^2 = p_{atm} - x_j\,\mathscr{H}_j$ when $p_{atm} - x_j\,\mathscr{H}_j = p_{atm}/100$. This suggests that the direct influence of flow, as measured via *We*, is negligible in lakes where (i) *U* is typically minute, and (ii) dissolved O_2 concentrations are below saturation. Thus, for example, the seasonally permanent physical gill supported by the pygmy backswimmer *Neoplea striola* (Gittelman 1975) is not significantly influenced by dynamic pressures.

The above scaling analysis illustrates why arthropods that take advantage of an external flow are most often found in well-aerated and relatively shallow streams. A case in point is the aquatic insect *Potamodytes tuberosus* (§ 1) that favours brisk overflows connecting stagnant flood pools and is only observed at depths of up to $\sim 5\,\mathrm{cm}$ (Stride 1954). We note that the respiratory bubble carried by *Potamodytes tuberosus* does not strictly qualify as a plastron because the bubble curvature is opposite to that shown in figure 3(*b*) so that

$$p_{bub} - p = \frac{2\sigma}{\bar{R}} > 0, \tag{5.4}$$

where $p = p_{atm} + \rho\,g\,H - Eu\,\rho\,U^2$ is the pressure on the bubble's exterior surface and $\bar{R} \simeq 1.5\,\mathrm{cm}$ is a characteristic bubble radius (Stride 1954). Therefore, the normal force balance on the bubble surface may be expressed as

$$Bo' + \Delta' - We' = -(\mathscr{Q}' + 2), \tag{5.5}$$

where

$$Bo' = \frac{\rho\,g\,H}{\sigma/\bar{R}}, \qquad We' = \frac{\mathrm{Eu}\,\rho\,U^2}{\sigma/\bar{R}}, \tag{5.6}$$

and

$$\mathscr{Q}' = \frac{q}{A\,\mathscr{J}_{O_2}\,(\sigma/\bar{R})}, \qquad \Delta' = \frac{p_{atm} - x_j\,\mathscr{H}_j}{\sigma/\bar{R}}. \tag{5.7}$$

Equation (5.5) can be satisfied provided $p_{O_2} > 0$. Thus, the (dimensional) respiration rate, *q*, and bubble surface area, *A*, must satisfy

$$x_{O_2}\,\mathscr{H}_{O_2}\,A\,\mathscr{J}_{O_2} > q. \tag{5.8}$$

Under representative flow conditions (i.e. $U \simeq 1\,\mathrm{m\,s^{-1}}$; Stride 1954), we find that $We' \gtrsim 2Bo'$. Because $\Delta \simeq 0$ in well-aerated water, this suggests that the dominant balance of terms in (5.5) is between We' and $\mathscr{Q}'$.

Potamodytes tuberosus appears to have specially designed femora and elytral tubercles that deflect the oncoming flow in the dorsal direction. As remarked by Stride (1954), this offers "protection to the anterior parts of the respiratory bubble" and minimizes the likelihood of the bubble being swept downstream. The elytral tubercles also ensure a rapid separation of the boundary layer from the insect's integument, which creates conditions favourable for the appearance of a cavitation bubble (Kundu 1990).

To further illustrate the significance of dynamic effects, we contrast the respiratory behaviour of *Potamodytes tuberosus* with the aquatic spider *Argyroneta aquatica* that occupies central and northern Europe and Asia. As explained by Schütz & Taborsky (2003), *Argyroneta aquatica* is able to survive underwater by virtue of a 'diving bell', consisting of an air bubble of approximate volume 1–3 ml enmeshed within a tightly woven web. As with *Potamodytes tuberosus*, this respiratory bubble is convex on the outside and is therefore also qualitatively different from a plastron. Because *Argyroneta aquatica* must affix its diving bell to aquatic plants or stones, it cannot occupy the brisk currents favoured by *Potamodytes tuberosus*. Consequently, the influence of dynamics is negligible and the respiratory bubble cannot be maintained indefinitely, obliging *Argyroneta aquatica* to make periodic ascents to the free surface to collect a fresh supply of air along its hydrophobic abdomen and legs. This air is then added to the respiratory bubble to make up for gas lost to diffusion and respiration.

5.2. *Enhanced boundary layer transport*

Even when *We* is relatively small, fluid flow may be important for two reasons. First, as described in detail by Hinton (1976), moving waters typically have a relatively high concentration of dissolved gases owing to mixing down from the surface. Second, the (mass diffusion) boundary layer thickness $\bar{\delta}_{O_2}$ is expected to decrease with increasing U. Supposing that mass transfer to and from a plastron is analogous at leading order to forced convection over a flat plate, one can apply the Blasius solution to show that

$$\bar{\delta}_{O_2} = \frac{\Upsilon\, \nu^{1/6}\, \widehat{D}_{O_2}^{1/3}\, \beta^{1/2}}{U^{1/2}} \left(1 - \frac{D}{\beta}\right)^{1/2}, \tag{5.9}$$

where ν is the kinematic viscosity and Υ is an $O(1)$ constant. Therefore, from the definition of $\mathscr{J}_{O_2}$ given by (3.4),

$$\mathscr{J}_{O_2} = \frac{\alpha_{O_2}\, \widehat{D}_{O_2}^{2/3}\, U^{1/2}}{\Upsilon\, \nu^{1/6}\, \beta^{1/2}\, (1 - D/\beta)^{1/2}}. \tag{5.10}$$

Thus larger flow velocities are associated with larger invasion coefficients and smaller dimensionless respiration rates, since $\mathscr{Q} \propto \mathscr{J}_{O_2}^{-1}$. Such boundary layer effects may account for the ventilation movements described in § 1 by which arthropods flap their limbs or antennae to enhance gas exchange. Similar factors explain the need of certain species of fish to remain in continual motion lest they suffocate due to inadequate gas exchange across their gills (Couzin & Krause 2003).

6. Discussion and conclusions

On a small scale, the ratio of surface area to volume necessarily increases, and surface effects become increasingly important; such is the case with plastron breathers.

The piliferous arthropod integument repels water to the extent that, when submerged, a Cassie state is maintained and the resulting air layer may serve as an external gill, exchanging O_2 and CO_2 with the surrounding water column (Ege 1918; Thorpe & Crisp 1947*a*,*b*,*c*; 1949; Vogel 2006). For the idealized, two-dimensional geometry of figure 3(*b*), we have identified the circumstances in which an arthropod may remain submerged indefinitely. Viable plastrons must satisfy two basic requirements: (i) that the Laplace pressure balance the pressure drop across the plastron interface, and (ii) that the plastron surface area be sufficiently large that the rate of O_2 uptake matches the arthropod's metabolic demands. Constraints (i) and (ii) in turn demand that the plastron pressure be sub-atmospheric in many cases of biological importance (see e.g. the measurements made by Stride 1954). As a result, plastron breathers do not depend on the intricate adaptations required by fish to breathe at high pressure (Vogel 2006).

Parameter regions in which plastron viability is assured are presented in figure 6, which shows the maximum and minimum dive depths as a function of the respiration rate, hydrophobic hair geometry and dissolved gas concentration. A tightly packed hair lattice composed of small-diameter hydrophobic hairs may prove disadvantageous in near-surface waters where the interface deflection is too small to facilitate O_2 and CO_2 exchange across the liquid–gas interface. The benefit of optimal water-repellency may thus be offset if the creature's respiration rate is too large. Our analysis allows us to rationalize a number of biological observations, including range of depths and corresponding hair lattice geometries available to plastron breathers, the diving behaviour of hibernating insects, the dependence of dive time on the concentration of dissolved O_2 and N_2, and the respiratory value of dynamic pressures and flapping movements.

The present analysis presents a number of avenues for further exploration. First, for free-swimming arthropods, the conditions for plastron viability ought to be coupled with an Archimedean equation that ensures that the arthropod's bulk density match that of the surrounding water despite the contribution of the plastron to its buoyancy. Such a requirement is not universal, however, because many plastron-bearing (e.g. *Haemonia mutica*, *Neoplea striola* – see § 4.3) and non-plastron-bearing (e.g. *Potamodytes tuberosus* – see § 5) aquatic arthropods are observed to rest along lake and river beds or cling to rocks and aquatic plants. Others, such as *Elmis maugei* and *Riolus cupreus* exploit the connection between the tracheal system and the plastron to 'float or sink at will, rising and falling in the water in rapid succession if necessary' (Thorpe & Crisp 1949). Moreover Gittelman (1975) and Matthews & Seymour (2006) indicate that the family of backswimmers *Notonectidae* are able to regulate their buoyancy by exchanging O_2 between their haemoglobin and plastron. The impact of this exchange on plastron dynamics has not, to our knowledge, been rigorously examined.

Secondly, the lattice geometry depicted schematically in figure 3 assumes an idealized array of rigid hydrophobic hairs. Although the two-dimensional model considered here is an appropriate leading-order description of real arthropods, variability of hair geometry across species has been documented by Thorpe & Crisp (1949). Following the discussions of Hinton (1976) and Bush *et al.* (2008), we have here assumed that the plastron hairs are effectively rigid; specifically, that the resistance to bending is large relative to both the capillary forces that could lead to lattice heterogeneities due to hair aggregation (Kralchevsky & Denkov 2001), and the hydrostatic pressure forces that could cause individual hairs to buckle. The relative magnitude of the resistance to bending and capillary forces is

prescribed by

$$G_1 = \frac{\text{elastic resistance}}{\text{capillary force}} = \frac{1}{32}\frac{D^3}{L^2\,\ell_e} \tag{6.1}$$

where L is the hair length, $\ell_e = \sigma/E$ is the elastocapillary length, $E \simeq 10^{11}$ dyn cm^{-2} is Young's modulus (Bico *et al.* 2004; Kim & Mahadevan 2006). For the species described in table 1 we find that G_1 varies between 2.2 (*Stenelmis crenata*) and 1.8×10^2 (*Haemonia mutica*), but is otherwise an $O(10)$ quantity, supporting the conclusion that the hydrophobic hairs are relatively inflexible under the influence of capillary forces. The relative magnitude of resistance to bending and the hydrostatic force acting over a single hair at a depth H is prescribed by

$$G_2 = \frac{\text{elastic resistance}}{\text{hydrostatic force}} = \frac{1}{32}\frac{D^2}{L^2}\frac{E}{\rho g H}. \tag{6.2}$$

For hairs with length-to-diameter aspect ratio $L/D = 10$, $G_2 \sim O(1)$ at a depth of 300 m, an inference consistent with that of Hinton (1976), who concluded that the plastron hairs should be stable to buckling at pressures less than 40 atm. As a caveat, we note that most hairs taper towards their tips, so these tips are most prone to deflection.

Thirdly, while plastrons are necessarily indicative of a Cassie state, we have implicitly assumed that this Cassie state is always energetically favourable relative to the fully wetted Wenzel state. We note that situations may arise in which Cassie states emerge instead of energetically favourable Wenzel states (Lafuma & Quéré 2003; Cao *et al.* 2007); however, the relevance of such metastable Cassie states to plastrons is unclear. More generally, if physical contact is made between the bubble interface and the arthropod surface, the integument may transition irreversibly from a Cassie to a Wenzel state (Lafuma & Quéré 2003; Reyssat 2007; Reyssat, Yeomans & Quéré 2008; Nosonovsky 2007). To avoid this life-threatening turn of events, the plastron lattice is often significantly over-designed relative to the minimum lattice height criteria of (2.5) and (2.6). For example, the plastron breathers *Aphelocheirus aestivalis* and *Macrelmis corisors* exhibit, respectively, centre-to-centre hair spacings $\beta = 0.5\,\mu$m and $\beta = 1.6 - 1.8\,\mu$m and plastron thicknesses $h = 6\beta$ and $h \simeq 9.5\beta$ (Thorpe & Crisp 1949; Hinton 1976; see table 1). Further stability may be offered by the vertical position of the liquid–gas–solid triple point, which is typically located along the underside of the hydrophobic hairs. At spatial scales well below the capillary length, it has been shown that attachment of the liquid–gas interface along the underside of a convex solid surface corresponds to a local minimum of surface free energy (Nosonovsky 2007).

We conclude by briefly addressing possible technological applications of the present theory. Shirtcliffe *et al.* (2006) recently conducted a novel experiment in which a cavity with a void volume of 2.5 cm^3 bound by a superhydrophobic methyltriethoxysilane sol-gel foam was submerged underwater. A chemical reaction inside the cavity consumed O_2 at a rate of approximately 0.25 ml h^{-1}. When placed in an aerated water bath, Shirtcliffe *et al.* (2006) found that the O_2 concentration inside the void approached a finite value. Using scaling arguments, Shirtcliffe *et al.* (2006) extrapolated their results and estimated that a diving chamber composed of similar material and having a planar area $A_p = 90\,\text{m}^2$ would be required to provide sufficient O_2 to meet the normal respiratory demands of a human.

The equations of § 4 provide an alternative metric for assessing the geometric demands of self-contained diving chambers. Suppose for example that a chamber,

β (μm)	U (m s^{-1})	$\mathscr{Q}$	$x_j \mathscr{H}_j / p_{atm}$	H_{max} (m)	H_{min} (m)
10	1	3.37	1	0.43	0.30
			3/4	0	0
	0.1	10.7	1	0	0
5	1	1.19	1	3.67	2.22
			3/4	0.90	0
			1/2	0	0
	0.1	3.77	1	0	0
1	1	0.106	1	28.44	0
			3/4	25.74	6.14
			1/2	20.38	3.55
			1/4	3.78	0
			0	0	0
	0.1	0.337	1	23.11	13.81
			3/4	17.28	11.23
			1/2	6.45	4.02
			1/4	0	0
	0.01	1.07	1	0	0

TABLE 2. Maximum and minimum dive depths, H_{max} and H_{min}, for a self-contained diving chamber of planar area $A_p = 90\,m^2$ with $D/\beta = 0.5$. Here, $\mathscr{Q}$ is the dimensionless respiration rate defined by (4.4*b*), D and β are the geometric parameters defined in figure 3(*b*), and $x_j \mathscr{H}_j / p_{atm}$ is the non-dimensional dissolved gas concentration. For the calculations summarized here, a normal human rate of O_2 consumption of $q = 1.6\,l\,s^{-1}$ is assumed (Linden 1999). The external flow speed, U, is presumed to modify the invasion coefficient, $\mathscr{J}_{O_2}$, according to (5.10), but is neglected in the normal force balance (5.1).

constructed of superhydrophobic material with an effective contact angle of $\theta = 170^\circ$, has a surface texture similar to the idealized two-dimensional geometry illustrated schematically in figure 3 with $D/\beta = 0.5$ and $A_p = 90\,m^2$. Then, our model yields estimates for the maximum and minimum dive depths that may be achieved for various hydrophobic post spacings, β, external flow speeds, U, and dissolved gas concentrations, $x_j \mathscr{H}_j$. Results are summarized in table 2, and indicate that while appreciable dive depths are possible, they require very fine micro-topography in combination with brisk flow speeds and well-aerated water. Under less ideal circumstances, device performance is compromised so that H_{max} is restricted to relatively modest values (e.g. $\lesssim 5\,m$) despite the diving chamber's large planar area. As the examples of table 2 make clear, the ability of humans to exploit plastron-breathing apparati is compromised by our large metabolic rate. Nevertheless, superhydrophobic plastron-bearing materials may find application in marine technology. As suggested by Shirtcliffe *et al.* (2006), submerged cavities consisting of specially designed hydrophobic material might provide the O_2 necessary to run fuel cells through a mechanism analogous to plastron respiration. These fuel cells could in turn supply power to small underwater vehicles as might find a variety of applications. Provided their power requirements are relatively modest, only a small flux of O_2 would be needed and therefore only a modest cavity surface area would be required. While additional factors such as surface bio-fouling (e.g. by algae or barnacles) would need to be considered for the implementation of such devices, the above analysis provides an initial step towards identifying the conditions favourable to their deployment.

Our study is a small step in seeking to rationalize a subtle biological adaptation, the geometry of arthropod integument. In considering living creatures that have been evolving for over 200 million years, it is tempting to assume that they are, from a strictly mechanical perspective, optimized. Be that as it may, it is not always clear what physics factors into this optimization. For example, the topology of the arthropod integument is constrained not only by its roles in water-repellency and plastron breathing, but also by the energetics of hair growth. Furthermore, the desirable dive depths are influenced by resource abundance, predation effects and light attenuation. The present analysis simply shows that respiratory requirements must be considered in rationalizing the topology of arthropod integument.

The authors extend their gratitude to K. O. Flynn, Dr M. J. Hancock, S. Ogelthorpe, M. Prakash, Dr D. Quéré and Dr S. Vogel whose thoughtful remarks improved the quality of the present discussion. J. W. M. B gratefully acknowledges the financial support of the National Science Foundation through grant CTS-0624830 and Career Grant CTS-0130465.

REFERENCES

Abdelsalam, M. E., Bartlett, P. N., Kelf, T. & Baumberg, J. 2005 Wetting of regularly structured gold surfaces. *Langmuir* **21**, 1753–1757.

Andersen, N. M. 1976 A comparative study of locomotion on the water surface in semiaquatic bugs (Insects, Hemiptera, Gerromorpha). *Vidensk. Meddr. Dansk. Naturh. Foren.* **139**, 337–396.

Andersen, N. M. 1977 Fine structure of the body hair layers and morphology of the spiracles of semiaquatic bugs (Insecta, Hemiptera, Gerromorpha) in relation to life on the water surface. *Vidensk. Meddr. Dansk. Naturh. Foren.* **140**, 7–37.

Andersen, N. M. & Polhemus, J. T. 1976 Water-striders (Hemiptera: Gerridae, Veliidae, etc.). In *Marine Insects* (ed. L. Cheng), pp. 187–224. A North Holland.

Barthlott, W. & Neinhuis, C. 1997 Purity of the sacred lotus, or escape from contamination in biological surfaces. *Planta* **202**, 1–8.

Bico, J., Roman, B., Moulin, L. & Boudaoud, A. 2004 Elastocapillary coalescence in wet hair. *Nature* **432**, 690.

Bico, J., Thiele, U. & Quéré, D. 2002 Wetting of textured surfaces. *Colloids Surf.* A **206**, 41–46.

Brocher, F. 1912*a* Reserches sur la respiration des insects aquatiques adultes – les elmides. *Ann. Biol. Lac.* **5**, 136–179.

Brocher, F. 1912*b* Reserches sur la respiration des insects aquatiques adultes – les haemonia. *Ann. Biol. Lac.* **5**, 5–26.

Brown, H. P. 1987 Biology of riffle beetles. *Annu. Rev. Entomol.* **32**, 253–273.

Bush, J. W. M. & Hu, D. L. 2006 Walking on water: Biolocomotion at the interface. *Annu. Rev. Fluid Mech.* **38**, 339–369.

Bush, J. W. M., Hu, D. L. & Prakash, M. 2008 The integument of water-walking anthropods: Form and function. *Adv. Insect Physiol.* **34**, 117–192.

Cao, L., Hu, H.-H. & Gao, D. 2007 Design and fabrication of mirco-textures for inducing a superhydrophobic behavior on hydrophilic materials. *Langmuir* **23**, 4310–4314.

Carbone, G. & Mangialardi, L. 2005 Hydrophobic properties of a wavy rough substrate. *Eur. Phys. J.* E **16**, 67–76.

Cassie, A. B. D. & Baxter, S. 1944 Wettability of porous surfaces. *Trans. Faraday Soc.* **40**, 546–551.

Chaui-Berlinck, J. G., Bicudo, J. E. & Monteiro, L. H. 2001 The oxygen gain of diving insects. *Respir. Physiol.* **128**, 229–233.

Chen, Y., He, B., Lee, J. & Patankar, N. A. 2005 Anisotropy in the wetting of rough surfaces. *J. Colloid Interface Sci.* **281**, 458–464.

Couzin, I. D. & Krause, J. 2003 Self-organization and collective behavior in vertebrates. *J. Adv. Study Behav.* **32**, 1–75.

Crisp, D. J. 1949 The stability of structures at a fluid interface. *Trans. Faraday Soc.* **46**, 228–235.

Dokulil, M. T. 2005 European alpine lakes. In *The Lake Handbook* (ed. P. E. O'Sullivan & C. S. Reynolds), vol. 2, pp. 159–178. Blackwell.

Doyen, J. T. 1976 Marine beetles (Coleoptera excluding Staphylinidae). In *Aquatic Insects* (ed. L. Cheng), pp. 497–520. North-Holland.

Ege, R. 1918 On the respiratory function of the air stores carried by some aquatic insects. *Z. Allg. Physiol.* **17**, 81–124.

Feng, Xi-Qiao & Jiang, Lei 2006 Design and creation of superwetting/antiwetting surfaces. *Adv. Mater.* **18**, 3063–3078.

Geankoplis, C. J. 1993 *Transport Processes and Unit Operations*. Prentice Hall.

de Gennes, P G, Brochard-Wyart, F & Quéré, D 2003 *Capillarity and Wetting Phenomena: Drops, Bubbles, Pearls and Waves*.Springer.

Gittelman, S. H. 1975 Physical gill efficiency and water dormancy in the pigmy backswimmer, Neoplea striola (Hemiptera: Pleidae). *Ann. Entomolo. Soc. Am.* **68**, 1011–1017.

Herminghaus, S. 2000 Roughness-induced non-wetting. *Europhys. Lett.* **52**, 165–170.

Hinton, H. E. 1976 Plastron respiration in bugs and beetles. *J. Insect Physiol.* **22**, 1529–1550.

Hinton, H. E. & Jarman, G. M. 1976 A diffusion equation for tapered plastrons. *J. Insect Physiol.* **22**, 1263–1265.

Holdgate, M. W. 1955 The wetting of insect cuticle by water. *J. Expl Biol.* **32**, 591–617.

Kim, H.-Y. & Mahadevan, L. 2006 Capillary rise between elastic sheets. *J. Fluid Mech.* **548**, 141–150.

Kralchevsky, P. A. & Denkov, N. D. 2001 Capillary forces and structuring in layers of colloid particles. *Curr. Opin. Colloid Interface Sci.* **6**, 383–401.

Kundu, P. K. 1990 *Fluid Mechanics*, 1st edn. Academic.

Lafuma, A. & Quéré, D. 2003 Superhydrophobic states. *Nature Materials* **2**, 457–460.

Lamoral, B. H. 1968 On the ecology and habitat adaptations of two intertidal spiders, Desis formidabilis and Amaurobioides africanus Hewitt at 'The Ísland' (Kommetjie, Cape Peninsula) with notes on the occurence of two other spiders. *Annu. Natal. Mus.* **20**, 151–193.

Linden, P. F. 1999 The fluid mechanics of natural ventilation. *Annu. Rev. Fluid Mech.* **31**, 201–238.

Matthews, P. G. D. & Seymour, R. S. 2006 Diving insects boost their buoyancy bubbles. *Nature* **441**, 171.

McMahon, T. & Bonner, J. T. 1985 *On Size and Life*. W. H. Freeman & Co.

Neinhuis, C. & Barthlott, W. 1997 Characterization and distribution of water-repellent, self-cleaning plant surfaces. *Annu. Bot.* **79**, 667–677.

Nosonovsky, M. 2007 Multiscale roughness and stability of superhydrophobic biomimetic interfaces. *Langmuir* **23**, 3157–3161.

Otten, A. & Herminghaus, S. 2004 How plants keep dry: A physicist's point of view. *Langmuir* **20**, 2405–2408.

Perez-Goodwyn, P. J. 2007 Anti-wetting surfaces in Heteroptera (Insecta): Hairy solutions to any problem. In *Functional Surfaces in Biology*. Springer.

Rahn, H. & Paganelli, C. V. 1968 Gas exchange in gas gills of diving insects. *Respir. Physiol.* **5**, 145–164.

Reysatt, M., Yeomans, J. M. & Quéré, D. 2008 Implacement of fakir drops. *Europhys. Lett.* **81**, 26006.

Reyssat, M. C. 2007 Splendeur et misère de l'effet lotus. PhD thesis, Université Pierre et Marie Curie.

de Ruiter, L., Wolvekamp, H. P., van Tooren, A. J. & Vlasblom, A. 1951 Experiments on the efficiency of the "physical gill" (Hydrous piceus l., Naucoris cimicoides l., and Notonecta glauca l.). *Acta Physiol. Pharmacol. Neerl.* pp. 180–213.

Schmidt-Nielsen, K. 1975 *Animal Physiology – Adaptation and Environment*. Cambridge University Press.

Schütz, D. & Taborsky, M. 2003 Adaptations to an aquatic life may be responsible for the reversed sexual size dimorphism in the water spider, argyroneta aquatica. *Ecol. Evol. Res.* **5**, 105–117.

Shirtcliffe, N. J., McHale, G., Newton, M. I., Perry, C. C. & Pyatt, F. Brian 2006 Plastron properties of a superhydrophobic surface. *Appl. Phys. Lett.* **89**, 104106.

Spence, J. R., Spence, D. H. & Scudder, G. G. 1980 Submergence behavior in *Gerris*: Underwater basking. *Am. Midl. Nat.* **103**, 385–391.

Stratton, G. E., Suter, R. B. & Miller, P. R. 2004 Evolution of water surface locomotion by spiders: a comparative approach. *Biol. J. Linn. Soc.* **81** (1), 63–78.

Stride, G. O. 1954 On the respiration of an aquatic african beetle, Potamodytes tuberosus Hinton. *Ann. Entomolo. Soc. Am.* **48**, 344–351.

Thorpe, W. H. 1950 Plastron respiration in aquatic insects. *Biol. Rev.* **25**, 344–390.

Thorpe, W. H. & Crisp, D. J. 1947*a* Studies on plastron respiration. Part I. The biology of Aphelocheirus [Hemiptera, Aphelocheiridae (Naucoridae)] and the mechanism of plastron retention. *J. Expl Biol.* **24**, 227–269.

Thorpe, W. H. & Crisp, D. J. 1947*b* Studies on plastron respiration. Part II. The respiratory efficiency of the plastron in Aphelocheirus. *J. Expl Biol.* **24**, 270–303.

Thorpe, W. H. & Crisp, D. J. 1947*c* Studies on plastron respiration. Part III. The orientation responses of Aphelocheirus [Hemiptera, Aphelocheiridae (Naucoridae)] in relation to plastron respiration; together with an account of specialized pressure receptors in aquatic insects. *J. Expl Biol.* **24**, 310–328.

Thorpe, W. H. & Crisp, D. J. 1949 Studies on plastron respiration. Part IV. Plastron respiration in the Coleoptera. *J. Expl Biol.* **26**, 219–260.

Vogel, S. 2006 Living in a physical world viii. Gravity and life in the water. *J. Biosci.* **31**, 309–322.

Wagner, P, Furstner, R, Barthlott, W & Neinhuis, C 2003 Quantitative assessment to the structural basis of water repellency in natural and technical surfaces. *J. Expl Bot.* **54**, 1295–1303.

Wenzel, R. N. 1936 Resistance of solid surfaces to wetting by water. *Ind. Engng Chem.* **28**, 988–994.